AD-A166 811   THE NEUTRON AND GAMMA-RAY SENSITIVITY OF AN   1/1
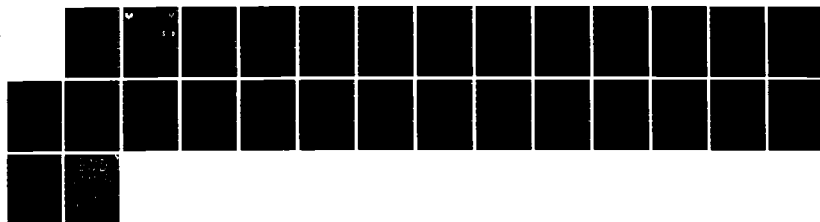   ARGON-FILLED ION CHAMBER(U) ARMY COMBAT SYSTEMS TEST
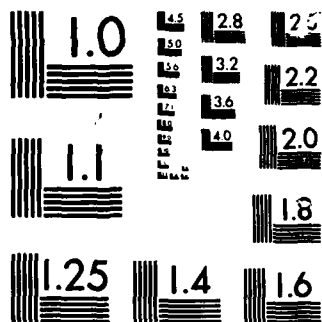   ACTIVITY (PROV) ABERDEEN PROVING GROUND MD
UNCLASSIFIED   C R HEIMBACH MAR 86 USACSTA-6360   F/G 18/4   NL

AD NO._____
TECOM PROJECT NO. 2-CO-430-APR-084
REPORT NO. USACSTA-6360

US ARMY
MATERIEL COMMAND

AD-A166 811

RESEARCH REPORT

THE NEUTRON AND GAMMA-RAY SENSITIVITY

OF

AN ARGON-FILLED ION CHAMBER

CRAIG R. HEIMBACH

NUCLEAR EFFECT DIRECTORATE

DTIC
ELECTE
APR 3 0 1986
S   D
D

U.S. ARMY COMBAT SYSTEMS TEST ACTIVITY
ABERDEEN PROVING GROUND, MD 21005-5059

MARCH 1986

Period Covered:
June to September 1985

Prepared For:
U.S. ARMY COMBAT SYSTEMS TEST ACTIVITY
ABERDEEN PROVING GROUND, MD 21005-5059

U.S. ARMY TEST AND EVALUATION COMMAND
ABERDEEN PROVING GROUND, MD 21005-5055

DISTRIBUTION UNLIMITED.

DTIC FILE COPY

86 4 30   023

DISPOSITION INSTRUCTIONS

Destroy this report when no longer needed. Do not return to the
originator.

DISCLAIMER STATEMENT

The views, opinions, and/or findings in this report are those of
the author(s) and should not be construed as an official Department
of th Army position, unless so designated by other official
documentation.

REPORT DOCUMENTATION PAGE	READ INSTRUCTIONS BEFORE COMPLETING FORM

1. REPORT NUMBER	2. GOVT ACCESSION NO.	3. RECIPIENT'S CATALOG NUMBER
TECOM Project 2-CO-430-APR-084	AD-A166 871	

4. TITLE (and Subtitle)	5. TYPE OF REPORT & PERIOD COVERED
THE NEUTRON AND GAMMA-RAY SENSITIVITY OF AN ARGON-FILLED ION CHAMBER	Research Report, June to September 1985
	6. PERFORMING ORG. REPORT NUMBER
	USACSTA-6360

7. AUTHOR(s)	8. CONTRACT OR GRANT NUMBER(s)
Craig R. Heimbach	None

9. PERFORMING ORGANIZATION NAME AND ADDRESS	10. PROGRAM ELEMENT, PROJECT, TASK AREA & WORK UNIT NUMBERS
U.S. Army Combat Systems Test Activity ATTN: STECS-NE Aberdeen Proving Ground, MD 21005-5059	None

11. CONTROLLING OFFICE NAME AND ADDRESS	12. REPORT DATE
Commander, USACSTA ATTN: STECS-NE Aberdeen Proving Ground, MD 21005-5059	March 1986
	13. NUMBER OF PAGES

14. MONITORING AGENCY NAME & ADDRESS(If different from Controlling Office)	15. SECURITY CLASS. (of this report)
None	Unclassified
	15a. DECLASSIFICATION DOWNGRADING SCHEDULE
	None

16. DISTRIBUTION STATEMENT (of this Report)

Distribution unlimited.

17. DISTRIBUTION STATEMENT (of the abstract entered in Block 20, if different from Report)

None

18. SUPPLEMENTARY NOTES

None

19. KEY WORDS (Continue on reverse side if necessary and identify by block number)

Ion chamber
Neutron sensitivity
Gamma-ray sensitivity
Cavity theory

20. ABSTRACT (Continue on reverse side if necessary and identify by block number)

In order to use an ion chamber accurately in a mixed neutron and gamma-ray field, its sensitivity to all components of the radiation must be known. The sensitivity of a commercial steel-walled, argon-filled ion chamber to neutrons and gamma rays of various energies has been measured and compared to calculated estimates. The ion chamber gives conservative results when used in an unknown field, and the overestimates can be quite large.

DD FORM 1473 EDITION OF 1 NOV 65 IS OBSOLETE

THE NEUTRON AND GAMMA-RAY SENSITIVITY OF
AN ARGON-FILLED ION CHAMBER

Craig R. Heimbach
Nuclear Effects Directorate
Combat Systems Test Activity
Aberdeen Proving Ground, MD 21005

and

Thomas Cousins and Bernard E. Hoffarth
Department of National Defence
Defence Research Establishment Ottawa
Ottawa, Ontario K1A 0Z4

ABSTRACT: In order to use an ion chamber accurately in a mixed
neutron and gamma-ray field, its sensitivity to all components of
the radiation must be known. The sensitivity of a commercial
steel-walled, argon-filled ion chamber to neutrons and gamma rays of
various energies has been measured and compared to calculated
estimates. The ion chamber gives conservative results when used in
an unknown field, and the overestimates can be quite large.

1. INTRODUCTION

    Ion chambers are often used in mixed neutron-gamma radiation
environments to measure the radiation kerma. They are typically
sensitive to both neutrons and gamma rays, but not with the same
efficiency. In order to interpret the ion chamber readings
correctly, one must understand how the ion chamber is responding
to each of these radiation components.

    The Nuclear Effects Directorate (NED) has acquired a
Reuter-Stokes model RSS-111 ion chamber in order to measure
gamma-ray tissue kerma in low-level radiation fields. This ion
chamber has the advantages of high sensitivity (down to a few
micro-Rad per hour), ruggedness, and portability. In order to use
this detector in the variety of radiation fields encountered by
the NED, however, it became necessary to calibrate this detector
as a function of both neutron and gamma-ray energies.

    The manufacturer of the detector (Reuter-Stokes) has supplied a
gamma-ray sensitivity function with the instrument (Fig. 1). This
was based on the calcluations and measurements of Ref. 1. No neutron

A-1

response was supplied, but Ref. 2 and 3, for example, indicated that there might be a substantial response to neutrons, especially at higher energies. Since the ion chamber was expected to respond in a spectrum-dependent manner for both neutrons and gamma rays, a calibration effort was undertaken.

The Reuter-Stokes RSS-111 ion chamber consists of a 12.7 cm radius spherical ion chamber filled with high-purity argon gas to a pressure of 25 atmospheres. The thickness of argon gas penetrated in one radius is 0.51 gm/cm**2. The wall of the ion chamber is a 0.30 cm thick type 304 stainless steel. For safety, this is then enclosed in another cubical case of 0.24 cm thick steel. The ion chamber is operated with the outer case in place, for a total steel thickness of 0.54 cm. (4.26 gm/cm**2).

2. CALCULATION OF SENSITIVITY

A calculation of the sensitivity of the RSS-111 to neutrons and gamma rays was performed prior to measurement for two reasons: First, calculated curves could be used in the selection of energies at which to calibrate; and, secondly, the calculated shape of the response function could be used to interpolate between measured points.

A. Gamma-ray Response

The ionization which is measured with the ion chamber occurs in the argon gas. This ionization has two sources: gamma-ray interactions in the gas generate electrons which are collected; and gamma-ray interactions in the steel walls generate electrons which penetrate into the gas and are then collected. The dominant mechanism depends upon the range of electrons in the gas. For long electron ranges, the ionization in the gas is primarily due to gamma interactions in the walls; for short electron ranges, the electrons in the gas are primarily due to gamma interactions in the gas itself.

One of the first things to be shown was that electrons generated outside the chamber could not penetrate to the interior. This is necessary for the ion chamber to be sensitive only to the gamma-ray environment, and not sensitive to incident electrons. This is done in Table 1, where the CSDA (Continuous- Slowing-Down Approximation) range of electrons in iron is shown to be less than the wall thickness of 4.26 gm/cm**2 for gamma rays of energies below 10 MeV. This is also sufficient thickness for charged particle equilibrium to be attained in the walls; i.e., the electron spectrum penetrating the gas from the walls is characteristic of iron. Gamma-ray spectra encountered in normal use at NED will not contain a significant amount of gamma rays of energy greater than 10 MeV.

Burlin general cavity theory as presented in Ref. 4 was used develop the gamma-ray sensitivity of the RSS-111. In this theory,

$$D(Fe) = (1/f) \star D(A)$$

where D(Fe) and D(A) are the doses deposited in iron and argon, respectively. f is the conversion factor relating the dose

deposited in argon, which is measured, to the dose deposited in a small sample of iron. To convert the iron kerma to tissue kerma, one multiplies by the ratio of mass energy absorption coefficients of tissue/iron for the energy of the incident gamma rays.

The conversion factor f is found from

$$f = d*s + (1-d)*(\mu/\rho)$$

where s is the ratio of mass stopping powers of argon/iron and (μ/ρ) is the ratio of mass energy absorption coefficients of argon/iron. d is a function of the electron range in the gas.

For a large electron range, d approaches unity, and the conversion factor f approaches the mass-stopping-power ratio. This is the normal Bragg-Gray relation for small-cavity ion chambers. For a small electron range, d approaches zero, and f approaches the mass energy absorption coefficient ratio. This is the appropriate limit for neglecting the effect of the walls of the ion chamber. For intermediate electron ranges, one has the appropriate weighted average of s and μ/ρ to give the correct calibration factor.

The expression used to calculate d is

$$d = \frac{1-\exp(-b*g)}{b*g}$$

where b is the effective mass attenuation coefficient for electrons in the gas, and g is the average path length of electrons in the gas cavity. These are somewhat difficult to calculate because there is a whole spectrum of electrons for even monoenergetic incident gamma rays, and because the average path length is dependent on the geometry of the ion chamber. For purposes of this calculation, the simplifiying approximation is made that the reciprocal of the electron range for electrons of energy of one-half the incident gamma-ray energy could be used for b. (This approximation fails outside the rane 1-5 MeV gamma, but does not greatly affect the calculated results.) Also, the average path length in the cavity (g) was taken to equal the chamber radius.

The above equations are based on the implicit assumption that there is no significant attenuation of the gamma-ray flux through the chamber. This is true for high-energy gamma rays, but not for low-energy gamma rays. A transmission factor of $T=\exp(-\mu(E)xD)$ was used to correct for gamma-ray attenuation through the shell. Here, $\mu(E)$ is the energy-dependent mass energy-absorption coefficient of iron, and D is the effective thickness of the sum of the two steel shells in gm/cm**2. The effective thickness is found from the actual thickness by considering the fact that the gamma rays strike the shells at various angles and thus pass through more material than the nominal (radial) thickness. The ratio of effective to nominal thickness varies somewhat with the angular distribution of the radiation and the attenuation of the shell. A ratio of 1.4, suitable for medium attenuation of isotropic radiation on a spherical shell, was used for these calculations. This will affect mainly the efficiency below 1 MeV.

3

The tissue kerma D(Ti) is found from the iron kerma D(Fe) from

$$D(Ti) = \frac{(\mu en/\rho)Ti}{(\mu en/\rho)Fe} * D(Fe)$$

Table 2 shows the calculation of the gamma-ray sensitivity of the RSS-111. Values of electron range and s were taken from Ref. 5, and values of μ/ρ were taken from Ref. 6. The efficiency at 1.2 MeV is normalized to unity because the chamber is calibrated in a Co-60 gamma-ray field.

Figure 2 shows the calculated gamma-ray response functions for three different effective thickness ratios of the shell (1.2, 1.4, and 1.6). Figure 3 compares the calculated response against the supplied response function. There are differences both at low and high energies. In radiation environments of interest to NED, only about 5% of the gamma-ray kerma is due to gamma rays below 200 kev, so that the differences at low energies may be neglected. The differences at high energies are significant.

B. Fast Neutrons

Burlin cavity theory can, with some difficulty, be adapted to find the neutron sensitivity of the RSS-111. As before,

$$D(Fe) = (1/f) * D(A),$$

but now

$$f = d*s + (1-d)*k.$$

s is now the ratio of stopping powers of the heavy charged particles which result from neutron interactions. k is the ratio of the kerma factors of the chamber wall and the filling gas, where a kerma factor is the amount of energy released per neutron/cm**2 in the given material. The calculation of d is similar to the electron case, except that the effective mass attenuation coefficient for heavy charged particles, and not for electrons, is used.

The primary difficulty in applying Burlin theory in this case is that there are several mechanisms of interaction of the neutrons with the chamber materials. One may have recoil particles, or neutron-generated protons, alphas, gammas, etc. Thus, finding the secondary-particle range and stopping power is quite difficult. The range for recoil protons will be used for estimating purposes, and the stopping power will be taken to be inversely proportional to the range. The energy of the recoil proton will be approximated to be less than the energy of the incident neutron by 3 MeV, the Q-value of the Fe-56(n,p) reaction.

To find the range of protons in argon, the Bragg-Kleeman relationship was used:

4

$$\frac{R \times \rho}{\sqrt{A}} = \text{Const}$$

where R is the range in cm, ρ is the density of the absorbing material, and A is the atomic number of the absorbing material. The range of protons in air (A=14.7) was taken from Ref 7.

The transmission factor for neutrons through the shell of the ion chamber is taken to equal 1.0 for all neutron energies. (In effect, this assumes the neutron transmission to be the same as CO-60 gamma-ray transmission. This is a good approximation compared to some of the others in the calculation of neutron sensitivity.)

The results of these calcultation are shown in Table 3 and in Figure 4. The sensitivity to neutrons turns out to be significant only at higher neutron energies, and does not vary much with the factor d.

C. Thermal Neutrons

The RSS-111 contains iron and argon, both of which are sensitive to thermal neutrons. The iron has a cross section of 2.55 barns and the argon has a cross section of 0.69 barns. Since the iron cross section is higher, and since there is more iron, the iron contributes the bulk of the sensitivity. For a thin shell of thickness X, NG,the number of gamma rays per cm**2 produced, is

$$NG = \frac{NA \times \rho \times \sigma \times X}{A} \times NTH$$

where NA is Avogadro's number, ρ is the shell density, σ is the cross section, A is the atomic weight, and NTH is the thermal neutron fluence. This reduces to NG = 0.25 x X x NTH for iron. An increase of a factor of two resulting from thermal-neutrons interacting with the walls on the way out as well as on the way in is canceled by a decrease of a factor of two resulting from the fact that half the gamma rays are directed away from the sensitive volume. The tissue kerma (K) may be found from the number of gamma rays by use of the mass energy-transfer coefficient $\mu en/\rho$ for tissue:

$$K = NG \times EG \times (\mu en/\rho)$$

where EG is the energy released on the form of gamma rays (7.6 MeV). Using a shell thickness of 0.54 cm, and conversion constants of 1.60E-6 erg/MeV and 100 erg/gm/Rad, gives a sensitivity for the RSS-111 of 2.87E-10 Rad per thermal neutron/cm**2. This may be compared against the thermal neutron sensitivity of a Geiger counter of 2.0E-10 Rad per thermal neutron/cm**2 (Ref. 8).

The shell thickness is not adjusted here for the average path length of thermal neutrons in the iron, as it was for low-energy gamma rays, but this should be partly compensated by the fact that

5

the gamma rays, being generated in the steel, have less steel to penetrate before escaping the shell. These gamma rays are therefore less likely to generate ions which may be collected in the gas volume.

The estimate made here is subject to large uncertainty, but it does indicate the necessity of measuring the thermal-neutron sensitivity of the RSS-111 for use in radiation fields encountered at the NED.

3. MEASURED SENSITIVITIES

The neutron and gamma-ray sensitivities of the ion chamber were experimentally determined by comparing the response of the chamber to the response of NE-213 and He-3 spectrometers in various radiation fields. These detectors were chosen because they give spectra, and because they can be used to obtain separate neutron and gamma-ray results. Bare and cadmium-covered BF-3 proportional counters were used to monitor the thermal-neutron fluence. Thus, the complete radiation environment could be determined.

For some of the measurements, a bismuth germanate gamma-ray spectrometer was used to monitor the gamma-ray fields, but these results were always related to NE-213 results, and not used directly.

The detectors had been previously calibrated against neutron and gamma-ray sources of known intensity. The NE-213 was used to measure neutrons when the energy was greater than 2.0 MeV, and the He-3 was used when the neutron energy was less than 2.0 MeV. The expected uncertainty in the NE-213 and He-3 kerma results is 5%.

Two gamma-ray sources, Cs-137 and Co-60, were used to calibrate the RSS-111 at .67 Mev and 1.2 MeV, respectively.

Another source of radiation used was the 3 MeV Van de Graaff particle accelerator at Defence Research Establishment Ottawa (DREO). The targets and associated reactions used here were:

(a) Thin (~20 µg/cm**2) LiF targets which produced low energy neutrons via the Li-7(p,n)Be-7 reaction. Additionally, such targets produced high-energy (~7 MeV) gamma rays in sufficient intensity to be useful.

(b) Thick (~1000 µg/cm**2) deuterium targets which produced mid-energy neutrons via the D(d,n)T reaction.

(c) Thick (~1000 µg/cm**2) tritium targets which produced high-energy (fusion) neutrons via the T(p,n)He-3 reaction.

All measured kermas are listed in Table 4.

A. Gamma Rays

The gamma-ray efficiency curve is determined from the data of part a of Table 4. For the first two points, there were no neutrons, so that the efficiency could be determined directly.

For the last point, the gamma rays were mixed with 0.8 MeV

6

neutrons. A borated-poly brick was used between the source and detectors to reduce the neutrons, but they could not be eliminated. However, the 15.0 micro-rad neutron kerma could be neglected because the expected neutron sensitivity at 0.8 MeV is small. Even if the estimate of neutron sensitivity from Table 3 were in error by a factor of 5, this would still be less than a 1% correction. Figure 5 shows the measured gamma-ray spectrum. Fig. 6 shows the same spectrum weighted by the energy content of the gamma rays. These show a large gamma-ray peak centered at 7.5 MeV. Assuming that the RSS-111 reading of 34.4 micro-rad is due to an actual gamma tissue kerma of 22.0 micro-rad plus a thermal-neutron response of 1.0 micro-rad gives a sensitivity factor of 1.52 at 7.5 MeV. The gamma results are plotted in Figures 7 and 8. As can be seen, these measurements validate the calculation.

No low-energy gamma-ray sources of sufficient intensity were available for a calibration below 0.5 MeV, so that portion of the response remains somewhat uncertain. For the spectra encountered at the NED, however, this is effect is of minor importance, as will be shown below.

B. Fast Neutrons

The fast-neutron response of the RSS-111 was determined by simultaneous measurement of the radiation coming from the DREO Van de Graaff. The RSS-111 reading was adjusted by subtracting the gamma-ray and thermal-neutron responses from the actual reading. The net result was then attributed to fast-neutron sensitivity.

In interpreting the data in Table 4 to obtain a neutron response function, the measured gamma-ray response function is used to adjust for gamma-ray sensitivity. The gamma-ray spectra as measured by NE-213 were integrated over the gamma response function of the RSS-111 to obtain an equivalent RSS-111 reading. This was then subtracted from the actual RSS-111 reading to find the neutron response. Next, the BF-3 monitored thermal-neutron response was subtracted. The fast-neutron response of the RSS-111 was then compared with the NE-213 or He-3 measured response to find the neutron sensitivity factor. Since the subtraction of the gamma-ray response from the total response of the RSS-111 left a relatively small residual, the propogated errors were quite large. The neutron results are plotted in Figure 9.

The differences between the measurement and the calculation are larger than with the gamma-ray results. This is not surprising, considering the rough estimates made in the neutron calculation. Fig. 10 shows the evaluated neutron sensitivity function.

C. Thermal Neutrons

The thermal-neutron sensitivity of the RSS-111 was measured by placing the ion chamber in a mixed fast-neutron, thermal-neutron, and gamma-ray field, and making measurements with and without a thermal-neutron absorbing material.

The radiation field was generated by placing a Cf-252 neutron source inside 5-inch diameter and 8-inch diameter polyethylene spheres. The thermal-neutron flux was monitored with bare and

7

cadmium-covered BF-3 proportional counters.

The thermal-neutron absorbing material was boron-containing rubber 1/8 inch thick. Its thermal-neutron attenuation properties were measured by making shielded and unshielded measurements of the BF-3 counters. Its gamma-ray attenuation properties were measured with a Cs-137 source. The fast-neutron attenuation properties were neglected for several reasons: the low neutron/gamma ratio expected for radiation coming out of the sphere, the low fast-neutron sensitivity of the RSS-111, and the thinness of the rubber.

The measured data is listed in Table 5. The data was analyzed as follows: The bare RSS-111 response is

$$RS(B) = G + TN$$

where G and TN are the portions of the RSS-111 response due to gamma rays and thermal neutrons, respectively. With the RSS-111 shielded with the borated rubber, the response is

$$RS(S) = 0.985 \times G + 0.14 \times TN$$

The borated rubber transmitted 98.5% of the gamma kerma and 14% of the thermal-neutron generated kerma. The response to thermal neutron is therefore

$$TN = \frac{1}{0.858} \left[RS(B) - \frac{RS(S)}{0.985} \right]$$

The thermal- neutron sensitivity was measured three times in order to obtain the variation of results with different neutron moderators and source-detector distances. The averaged value of 2.63E-10 R/n-cm**2 is to be used for thermal neutrons. The largest error in this result is associated with the gamma-ray attenuation properties of the neutron shield. The overall accuracy is unlikely to be better than 20%.

4. APPLICATION

Knowledge of the energy response of the ion chamber allows a better interpretation of measured data. For example, the RSS-111 ion chamber was used to measured the radiation field at 170 m from the NED reactor. The neutron and gamma-ray spectra are shown in Figs. 11 and 12, respectively. Integrating over the response curves, one finds a gamma-ray sensitivity correction factor of 1.16. The neutron response is calculated to be only 1% of the gamma response, so it may be neglected. The adjustments for thermal neutron response and for gamma spectral response are given in Table 6. There is a 21% correction for thermal-neutron sensitivity and a further 16% correction for gamma-ray spectrum sensitivity which combine to give an overall reduction of 32% in the actual gamma-ray kerma as compared to the RSS-111 reading. The adjusted RSS-111 response agrees well with the NE-213 measured gamma-ray kerma.

8

Gamma-ray correction factors for other fields of interest to NED are listed in Table 7. In no case did using different low-energy transmission factors (see Fig. 2) change the computed gamma-ray correction factors by more than 1%. The corrections for fast neutrons were small, except for the 14 MeV field, but thermal neutrons had a significant contribution to the RSS-111 readings in all cases.

5. CONCLUSIONS

Since the gamma-ray sensitivity is always greater than or equal to the sensitivity at the calibration energy, the RSS-111 will always read high. Any neutron response will only add to the indicated result, so that the RSS-111 may be used as a conservative estimator of the gamma-ray kerma. In a field with many high-energy gamma rays, or with a dominating neutron component, especially of high-energy or thermal neutrons, the uncorrected RSS-111 response could be so high as to be misleading with respect to the true gamma kerma.

9

REFERENCES

1. "High Pressure Argon Ionization Chamber Systems For the
   Measurement of Environmental Radiation Exposure Rates",
   J.A. DeCampo, H.L. Beck, and P.D. Raft, HASL-260 (Dec 1972)

2. "Neutron Dosimetry for Biology and Medicine", ICRU Report 26 (1971)

3. "Neutron/Gamma Dose Separation by the Multiple Ion Chamber
   Technique",S.J. Goetsch, DOE/EV/01105-T2 (1983)

4. "Thermoluminescent Radiation Dosimetry", Y.S. Horowitz in
   "Thermoluminescence and Thermoluminescent Dosimetry", Vol. II,
   Y.S. Horowitz, Ed., CRC Press (1984)

5. "Stopping Powers for Electrons and Positrons", ICRU Report 37,
   (1984)

6. "X-Ray and Gamma-Ray Interactions", R.D. Evans in Radiation
   Dosimetry, Attix, Roesch, Tochlin, Ed., second edition, vol 1 (1968)

7. "CRC Handbook of Radiation Measurement and Protection",Section
   A, VI, "Physical Science and Engineering Data", CRC Press,
   Inc., (1978)

8. "A Geiger-Müller Gamma-Ray Dosimeter with Low Neutron Sensitivity",
   E.B. Wagner and G.S. Hurst, Health Physics,V5,20-26 (1961)

11

TABLE 1. RANGE IN IRON OF ELECTRONS RESULTING FROM GAMMA RAYS

GAMMA-RAY ENERGY (MEV)	AVERAGE COMPTON- RECOIL ELECTRON ENERGY (MEV) (a)	CSDA RANGE IN IRON (gm/cm**2) (b)
0.01	.0002	.0000
0.05	.0040	.0001
0.10	.0138	.0007
0.15	.0272	.0024
0.20	.0432	.0052
0.30	.0809	.0150
0.50	.171	.0512
0.60	.221	.0882
0.80	.327	.138
1.00	.440	.212
1.50	.742	.426
2.00	1.061	.661
3.00	1.731	1.15
4.00	2.428	1.64
6.00	3.864	2.62
8.00	5.338	3.53
10.00	6.835	4.38

(a) Ref. 6.
(b) Ref. 5.

TABLE 2. CALCULATION OF GAMA-RAY SENSITIVITY OF THE RSS-111

GAMMA ENERGY (MEV)	ELECTRON ENERGY (MEV)	CSDA RANGE (g/cm**2)	d	s(A/Fe)	μ/ρ(A/Fe)	f
0.05	.025	.0019	0	1.06	.30	.30
0.06	.03	.0026	0	1.05	.29	.29
0.07	.035	.0034	.01	1.05	.30	.31
0.08	.04	.0043	.01	1.05	.31	.32
0.09	.045	.0052	.01	1.05	.32	.33
0.10	.05	.0063	.01	1.05	.33	.34
0.15	.075	.0125	.02	1.04	.46	.47
0.20	.10	.0204	.04	1.04	.61	.63
0.30	.15	.0398	.08	1.04	.83	.85
0.40	.20	.0631	.12	1.04	.89	.91
0.50	.25	.0892	.17	1.04	.92	.94
0.60	.30	.117	.23	1.04	.94	.96
0.80	.40	.179	.33	1.04	.96	.99
1.00	.50	.244	.42	1.04	.96	.99
1.50	.75	.316	.50	1.05	.97	·1.01
2.00	1.00	.594	.67	1.05	.96	1.02
3.00	1.50	.948	.77	1.06	.94	1.03
4.00	2.00	1.29	.83	1.07	.91	1.04
5.00	2.50	1.63	.86	1.07	.89	1.04
6.00	3.00	1.96	.88	1.08	.87	1.05
8.00	4.00	2.59	.91	1.09	.85	1.07
10.00	5.00	3.19	.92	1.10	.83	1.08

GAMMA ENERGY (MEV)	f	μ/ρ(Fe/Tiss)	T	RSS-111 sensitivity
0.05	.30	29.23	.0001	0.00
0.06	.29	30.03	.0032	0.04
0.07	.31	22.5	.0248	0.24
0.08	.32	15.80	.0847	0.59
0.09	.33	12.3	.200	0.84
0.10	.34	8.55	.271	1.09
0.15	.47	2.94	.615	1.18
0.20	.63	1.67	.744	1.09
0.30	.85	1.05	.819	1.01
0.40	.91	.94	.832	0.97
0.50	.94	.89	.838	0.97
0.60	.96	.87	.843	0.98
0.80	.99	.85	.850	0.99
1.00	.99	.85	.855	1.00
1.50	1.01	.84	.868	1.02
2.00	1.02	.85	.877	1.06
3.00	1.03	.90	.885	1.14
4.00	1.04	.97	.888	1.24
5.00	1.04	1.04	.889	1.33
6.00	1.05	1.10	.888	1.42
8.00	1.07	1.23	.885	1.62
10.00	1.08	1.33	.883	1.76

TABLE 3. CALCULATION OF NEUTRON SENSITIVITY OF THE RSS-111

NEUTRON ENERGY (MEV)	PROTON ENERGY (MEV)	CSDA RANGE (g/cm**2)	d	s(A/Fe)	k(A/Fe)	f
0.10	--	--	.00	1.18	0.82	0.82
0.30	--	--	.00	1.18	1.42	1.42
0.50	--	--	.00	1.18	0.71	0.71
0.70	--	--	.00	1.18	1.23	1.23
1.00	--	--	.00	1.18	1.72	1.72
1.50	--	--	.00	1.18	1.72	1.72
2.00	--	--	.00	1.18	2.04	2.04
3.00	--	--	.00	1.18	1.80	1.80
4.00	1.00	.006	.01	1.18	1.55	1.53
5.00	2.00	.014	.03	1.18	1.20	1.20
7.00	4.00	.046	.05	1.18	0.78	0.82
9.00	6.00	.093	.18	1.18	0.67	0.83
11.00	8.00	.155	.29	1.18	0.57	0.75
13.00	10.00	.231	.40	1.18	0.52	0.79
15.00	12.00	.325	.50	1.18	0.71	0.94
17.00	14.00	.422	.58	1.18	0.76	1.00

NEUTRON ENERGY (MEV)	f	k(Fe/Tiss)	RSS-111 sensitivity
0.10	0.82	.003	.004
0.30	1.42	.003	.002
0.50	0.71	.005	.007
0.70	1.23	.005	.004
1.00	1.72	.005	.003
1.50	1.72	.008	.005
2.00	2.04	.009	.004
3.00	1.80	.011	.006
4.00	1.53	.013	.008
5.00	1.20	.015	.012
7.00	0.82	.022	.027
9.00	0.83	.033	.040
11.00	0.75	.043	.057
13.00	0.79	.056	.071
15.00	0.94	.071	.075
17.00	1.00	.088	.088

TABLE 4. MEASURED KERMA

a. Gamma-ray sensitivity calibration.

Gamma-ray Energy(MeV)	0.67	1.2	7.5
Gamma-ray Source	Cs-137	Co-60	p-LiF
Neutron Energy(MeV)	–	–	0.8
Fast-neutron Kerma(μR)	–	–	15.0
Thermal-neutron kerma(μR)	–	–	1.0
RSS-111 Kerma(μR)	240.5	230.4	34.4
NE-213 Gamma Kerma(μR)	236.2	228.0	22.0
Gamma-ray Sensitivity	1.02	1.01	1.52

b. Fast-neutron sensitivity calibration.

Neutron Energy(MeV)	0.80	4.1	14.0	16.7
Neutron Source	p-Li	D-D	D-T	D-T
RSS-111 Kerma(μR)	22.3	97.3	92.0	134.5
NE-213 Gamma Kerma(μR)	13.6	70.1	40.5	74.6
NE-213 Gamma Kerma, Adj. for RSS-111 Sens.(μR)	16.4	85.0	49.3	90.8
BF-3 Monitored Thermal-neutron sens.(μR)	5.5	6.4	2.3	3.2
Net RSS-111 Resp.(μR)	0.4	5.9	40.4	40.5
Fast-Neutron Kerma(μR)	217.0	1890.0	709.0	1280.0
Fast-Neutron Sensitivity	0.002	0.003	0.057	0.032

TABLE 5. DATA FOR THERMAL-NEUTRON SENSITIVITY OF THE RSS-111

Cf-252 cover source-detector distance	5-in 126 cm	5-in 200 cm	8-in 80 cm
RSS-111 (bare) (μR/hr)	333	123	402
RSS-111 (covered) (μR/hr)	313	111.5	379
Thermal-Neutron Sens.(μR/hr)	17.7	11.4	21.2
Thermal-Neutron Flux (n/cm^2-hr)	71400	43300	76600
sensitivity factor (R/n-cm^2)	2.48E-10	2.63E-10	2.77E-10

Average thermal neutron sensitivity factor = 2.63E-10 R/n-cm^2 (20%).

TABLE 6. EXAMPLE OF RSS-111 CORRECTIONS: 170M FROM NED REACTOR

RSS-111 Reading (μR/kwhr)	24.0
Thermal-Neutron Flux (n/cm^2-kwhr)	18,990.
RSS-111 Thermal-Neutron Correction (μR/kwhr)	5.0
RSS-111 Response due to gammas (μR/kwhr)	19.0
Rss-111 Adjusted for gamma response (μR/kwhr)	16.3
Actual gamma kerma at 170m (μR/kwhr)	16.5+-0.5

TABLE 7. RSS-111 CORRECTION FACTORS (a)

GAMMA-RAY ENVIRONMENT	CALCULATED RSS-111 CORRECTION FACTOR
170 m Free-field (b)	0.86
400 m Free-field (b)	0.86
1080 m Free-field (b)	0.85
M60A1 Turret (170m) (b)	0.73
400 m 14 MEV (c)	0.82

(a) Multiply this factor times RS-111 results, after
   subtracting neutron sensitivity, to find gamma-ray kerma.
(b) Distance from NED fast-burst reactor.
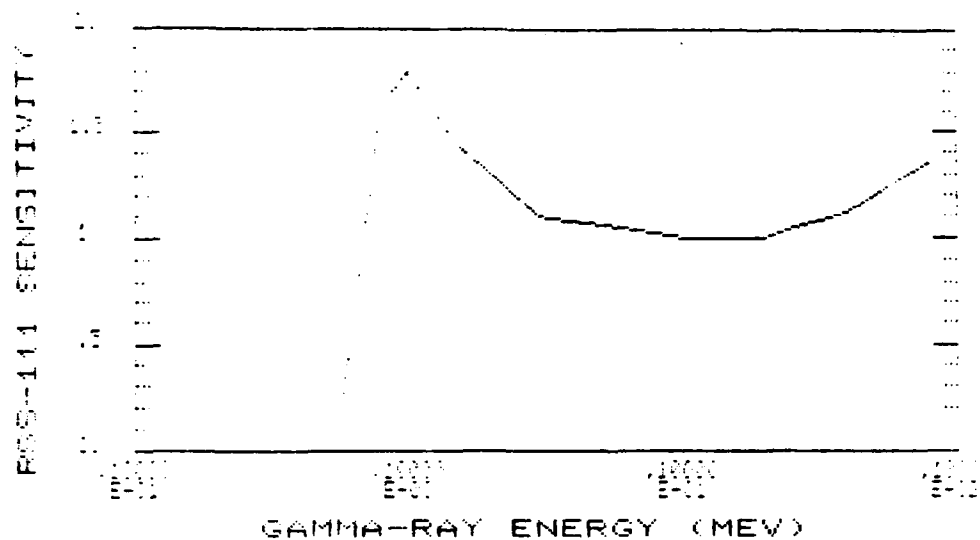(c) Distance from ETCA 14 MEV generator.

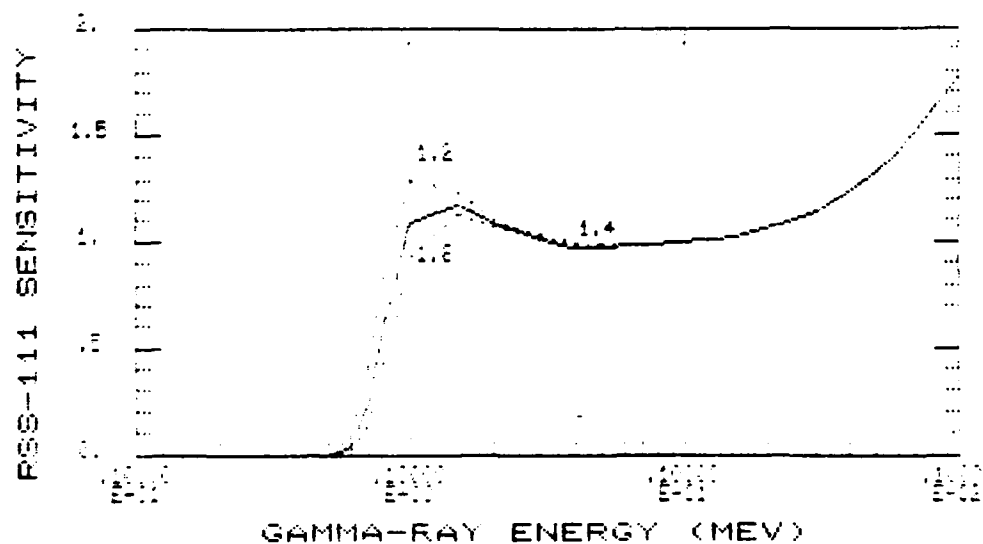Figure 1.   Reuter-Stokes supplied RSS-111 gamma-ray sensitivity.

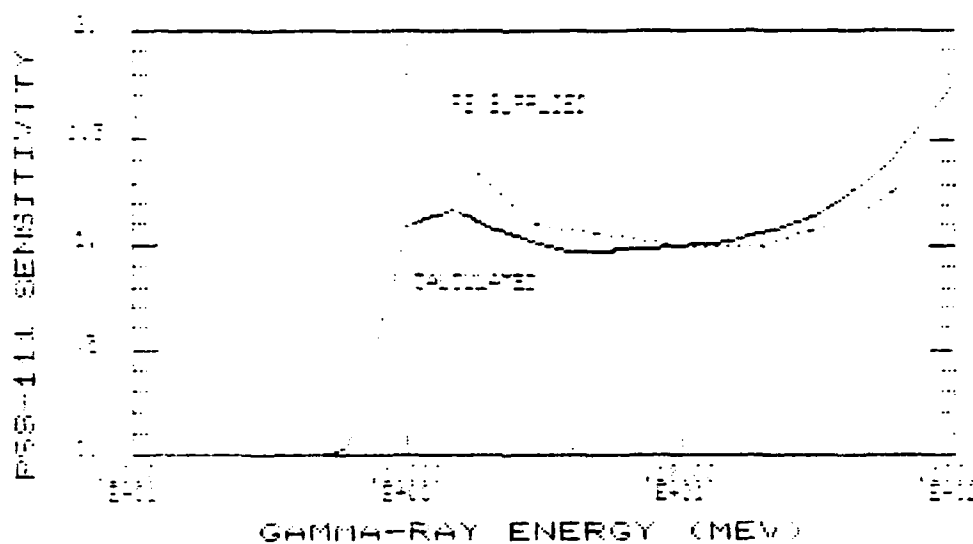Figure 2.   Calculated RSS-111 gamma-ray sensitivity.

18

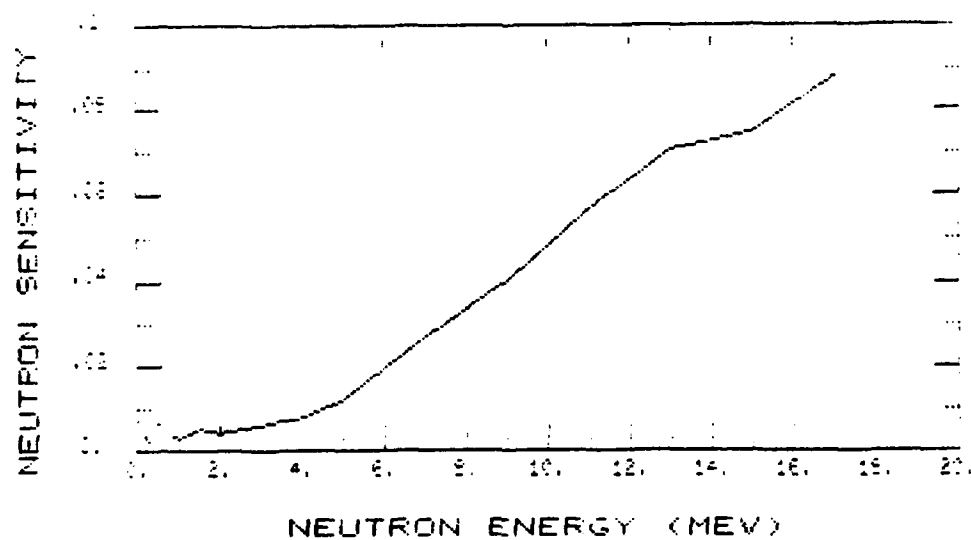Figure 3. Comparison of supplied and calculated gamma-ray sensitivities.

Figure 4. Calculated RSS-111 neutron sensitivity.
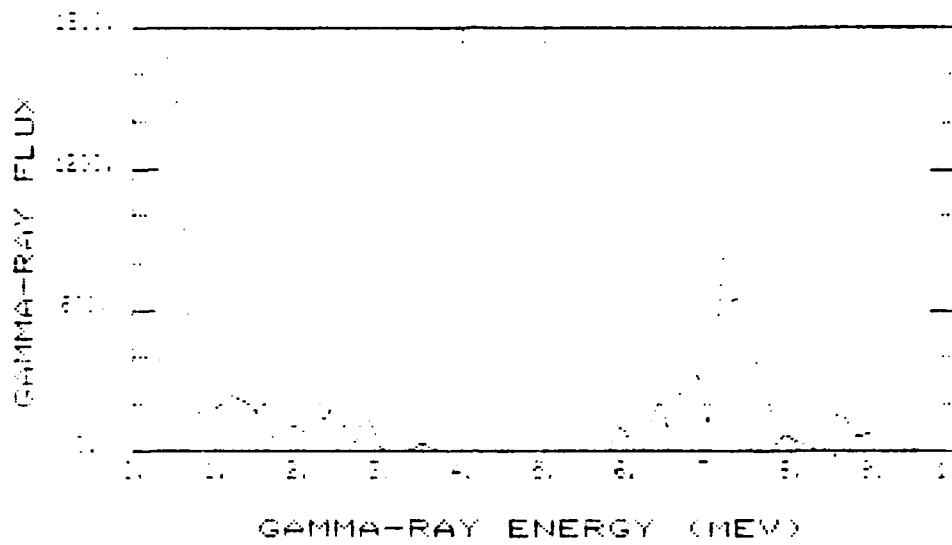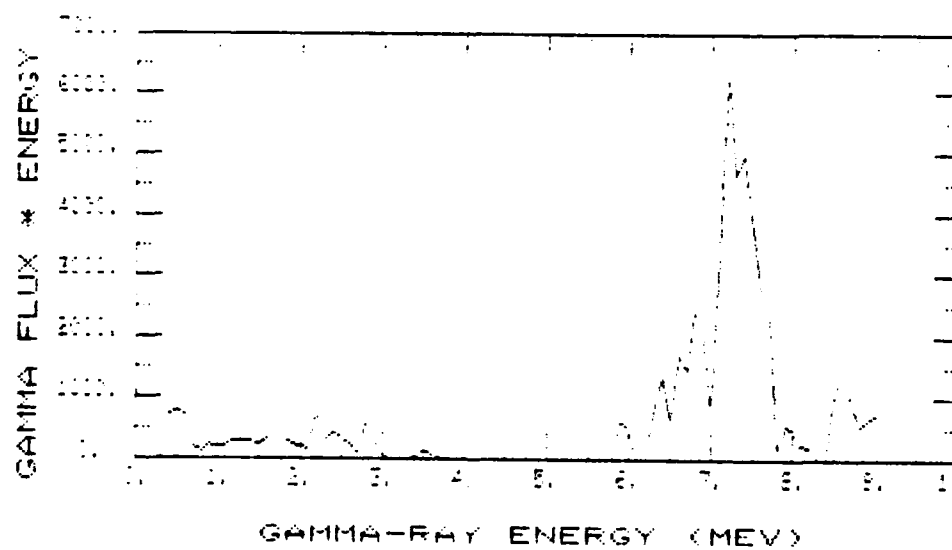
19

Figure 5. p-LIF gamma-ray spectrum.
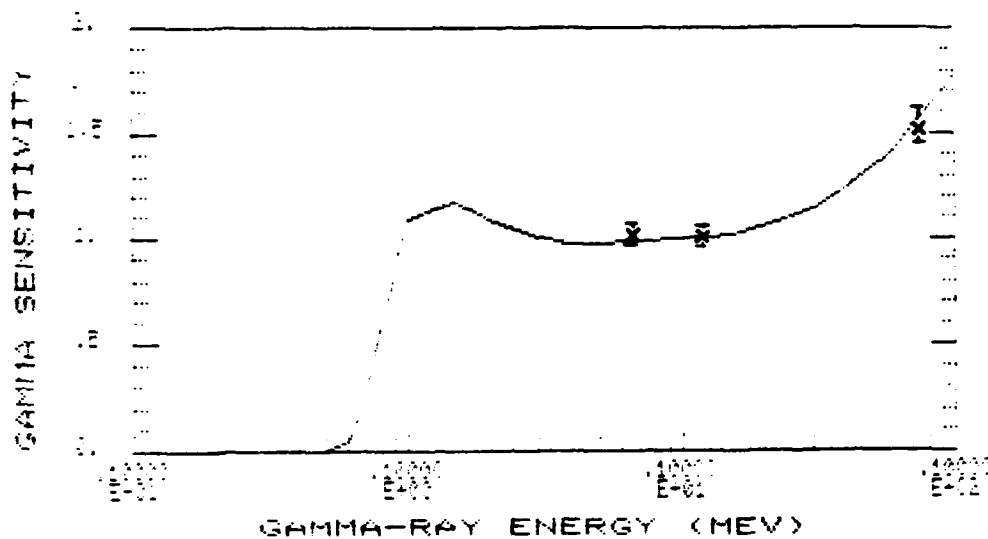

Figure 6. Energy-weighted p-LIF gamma-ray spectrum.

20

Figure 7. Comparison of measured and calculated gamma-ray sensitivities (logarithmic energy scale).
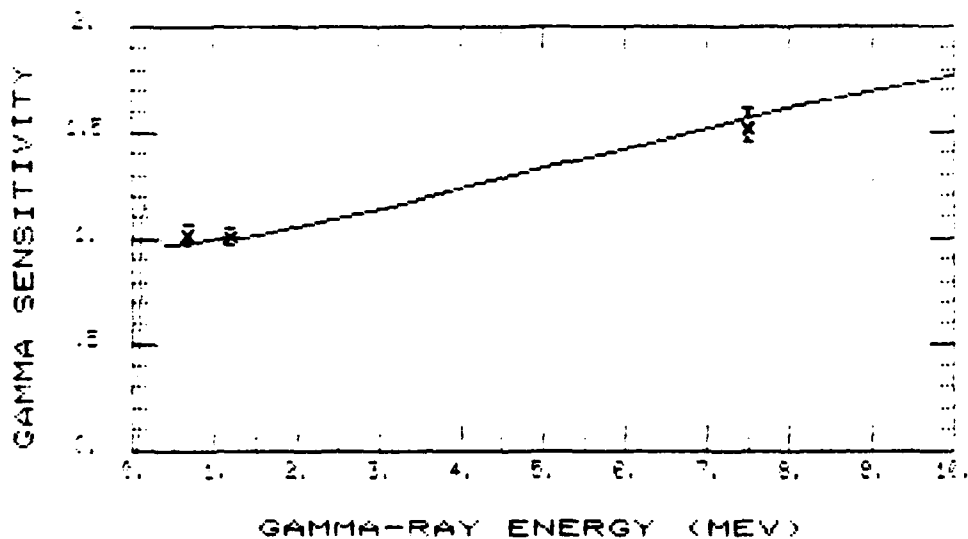

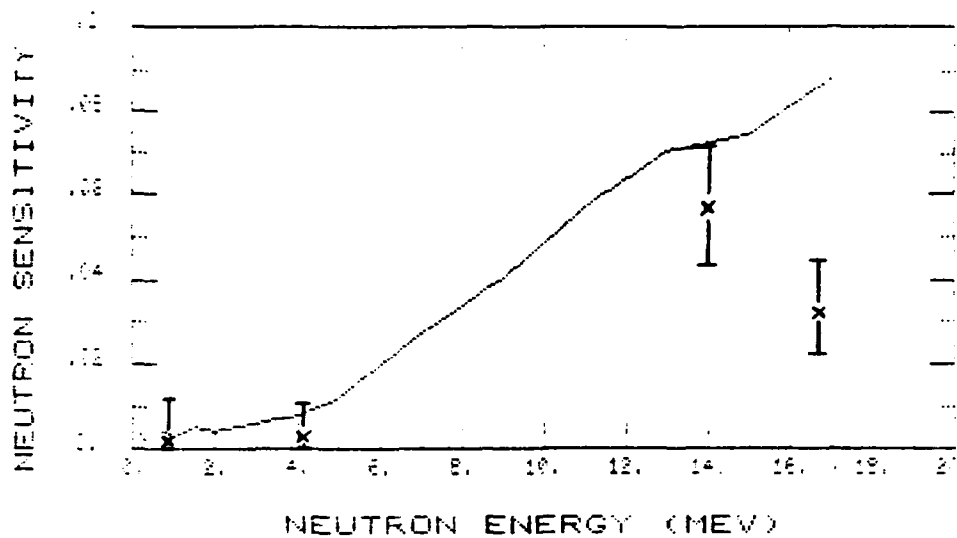Figure 8. Comparison of measured and calculated gamma-ray sensitivities (linear energy scale).

21

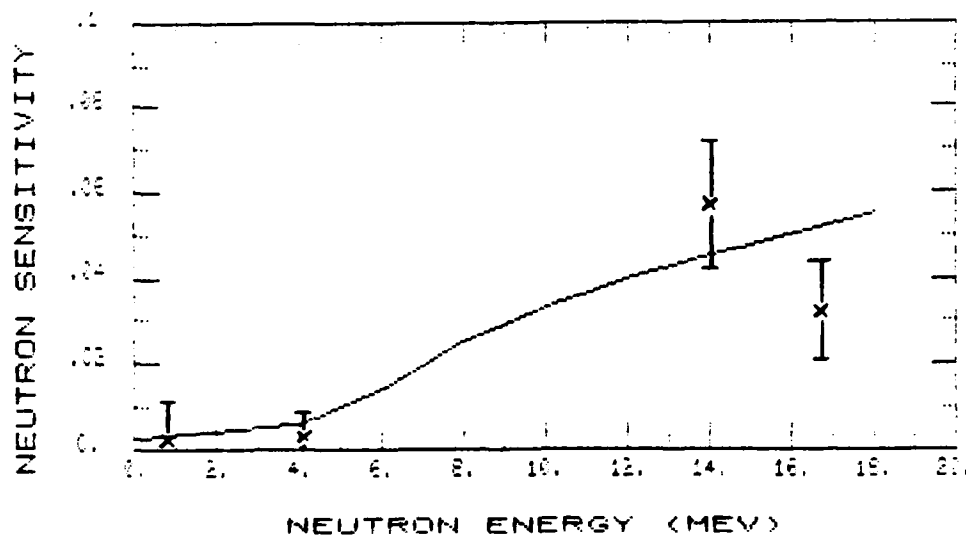Figure 9. Comparison of measured and calculated neutron sensitivities.
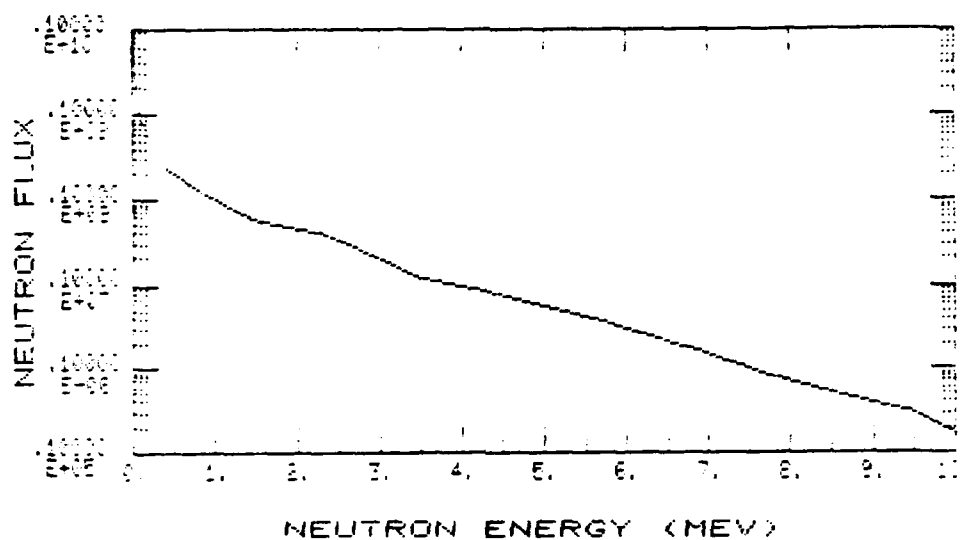

Figure 10. Evaluated neutron sensitivity of RSS-111.
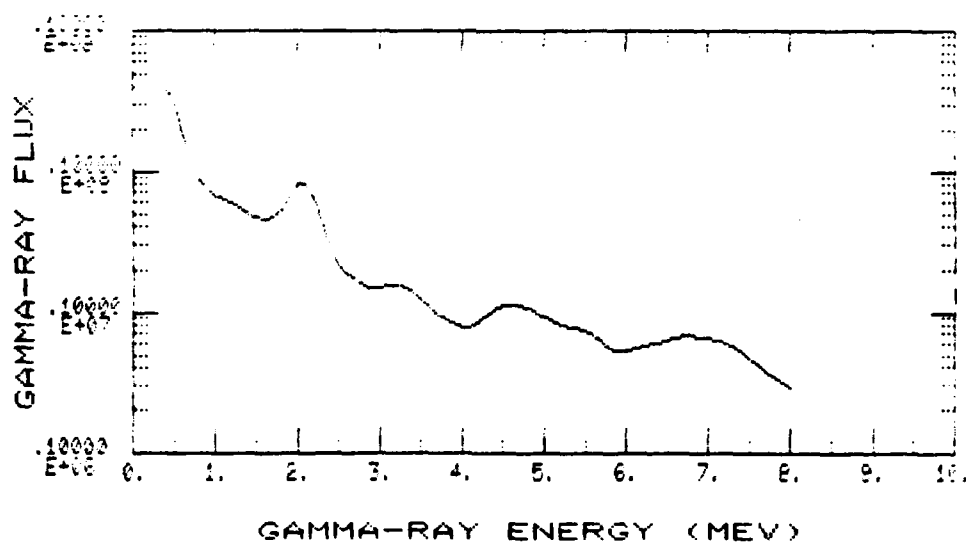
22

Figure 11. 170m neutron spectrum.

Figure 12. 170m gamma-ray spectrum.

23

DISTRIBUTION LIST

Addressee	No. of Copies
Commander U.S. Army Test and Evaluation Command ATTN: AMSTE-TO-H Aberdeen Proving Ground, MD 21005-5055	1
Commander U.S. Army Harry Diamond Laboratories ATTN: DELHD-NT, R. Bostak 2800 Powder Mill Road Adelphi, MD 20783-1197	a5
Commander U.S. Army Foreign Science and Technology Center ATTN: AMXST-FMO 220 Seventh Street, NE Charlottesville, VA 22901-5396	1
Director Defense Nuclear Agency ATTN: RATN, Dr. D. Auton Washington, DC 20305	1
Director U.S. Army Nuclear and Chemical Agency ATTN: MONA-WE MONA-ZB, C. N. Davidson 7500 Backlick Road, Building 2073 Springfield, VA 22150	1 1
Director Armed Forces Radiobiology Research Institute ATTN: CDR G. Zeman Building 42, NNMC Bethesda, MD 20014	1

a One copy to: Dr. Ludwig Schanzler
                Wehrwissenschaftliche Dienststelle
                  Der Bundeswehr Fur ABC-Schutz
                3042 Munster, Germany

One copy to: Establissement Technique Central
                De L'Armement
              ATTN: M.J. Laugier
              94114 Arcuil Cedex, France

One copy to: Colonel Amat
              Delegation Generale Pour L'Armement
              Bureau Dret/SDA, NBC 26
              Bd Victor, 75996 Paris Armees, France

25

Addressee	No. of Copies

Headquarters
U.S. Army Combat Surveillance and Target
  Acquisition Laboratory
ATTN: DELCS-K, Dr Groeber   1
       DELCS-K, S. Kronenberg   1
Fort Monmouth, NJ 07703

National Bureau of Standards Center for Radiation
  Research
ATTN: Mr. D. McGarry   1
       Dr. C. Eisenhower   1
Washington, DC 20234

University of California
Lawrence Livermore Laboratory
ATTN: William E. Loewe, L-10   1
       D.E. Hankins   1
Livermore, CA 94550

Oak Ridge National Laboratory
ATTN: Dr. J. Pace, III   1
       Dr. D. Trubey   1
       Dr. L. Holland   1
Oak Ridge, TN 37830

Science Applications, Inc.
ATTN: Dr. W. Scott   1
PO Box 2351
La Jolla, CA 92038

Science Applications, Inc.
ATTN: Dr. Dean C. Kaul   1
1701 E. Woodfield Road
Suite 819
Schaumburg, IL 60195

RDA, Inc.
ATTN: Dr. J. Markhum   1
4640 Admiralty Way
Marina del Rey, CA 90291

California Institute of Technology
ATTN: Dr. Robert F. Christy   1
Pasadena, CA 91125

Los Alamos National Laboratory
ATTN: Guy Estes   1
Mail Stop 226
Los Alamos, NM 87545

Addressee	No. of Copies

Naval Surface Weapons Center
ATTN: Gordon Riel   1
Code R41
White Oak, MD 20910

Reuter-Stokes, Inc.
ATTN: D. McCormick   1
18530 South Miles Parkway
Cleveland, OH 44128

Los Alamos National Laboratory
ATTN: A. E. Evans   1
PO Box 1663
Los Alamos, NM 87545

Kaman Tempo
ATTN: DASIAC (F. Wimenitz)   1
2560 Huntington Ave., Suite 500
Alexandria, VA 22303

Feren C. Hajnal
DOE/EML   1
376 Hudson Street
New York, NY 10014

Director
U.S. Army Ballistic Research Laboratory
ATTN: SLCBR-VL-T, D. Rigotti   b2
       SLCBR-VL-I, Dr. A. E. Rainis   1
       SLCBR-VL-I, H. Caton   2
       SLCBR-DD-T (STINFO)   2
Aberdeen Proving Ground, MD 21005-5066

Commander
U.S. Army Combat Systems Test Activity
ATTN: STECS-AD-A   1
       STECS-RM-T   1
       STECS-NE   20
Aberdeen Proving Ground, MD 21005-5059

Administrator
Defense Technical Information Center
ATTN: DDA   2
Cameron Station
Alexandria, VA 22304-6145

bOne copy to: Dr. T. Cousins
             Dept of National Defence
             Defence Research Establishment, Ottawa
             Ottawa, Ontario, Canada

Distribution unlimited.

END
FILMED

5-86

DTIC